

Real-time visualization of cytoplasmic calpain activation and calcium deregulation in acute glutamate excitotoxicity

Akos A. Gerencser,^{*,1} Karla A. Mark,^{*,1} Alan E. Hubbard,^{*,†} Ajit S. Divakaruni,^{*} Zara Mehrabian,^{‡,§} David G. Nicholls^{*} and Brian M. Polster^{*,‡,§,¶}

^{*}Buck Institute for Age Research, Novato, California, USA

[†]School of Public Health, University of California, Berkeley, California, USA

[‡]Department of Anesthesiology, University of Maryland School of Medicine, Baltimore, Maryland, USA

[§]Trauma and Anesthesiology Research Center, University of Maryland School of Medicine, Baltimore, Maryland, USA

[¶]Program in Neuroscience, University of Maryland School of Medicine, Baltimore, Maryland, USA

Abstract

Although calpain (EC 3.4.22) protease activation was suggested to contribute to excitotoxic delayed calcium deregulation (DCD) via proteolysis of Na⁺/Ca²⁺ exchanger 3 (NCX3), cytoplasmic calpain activation in relation to DCD has never been visualized in real-time. We employed a calpain fluorescence resonance energy transfer substrate to simultaneously image calpain activation and calcium deregulation in live cortical neurons. A calpain inhibitor-sensitive decline in fluorescence resonance energy transfer was observed at 39 ± 5 min after the occurrence of DCD in neurons exposed to continuous glutamate (100 μM). Inhibition of calpain by calpeptin did not delay the onset of DCD, recovery from DCD-like reversible calcium elevations, or cell death despite inhibiting

α-spectrin processing by > 90%. NCXs reversed during glutamate exposure, the NCX antagonist KB-R7943 prolonged the time to DCD, and significant NCX3 cleavage following 90 min of glutamate exposure was not observed. Our findings suggest that robust calpain activation associated with acute glutamate toxicity occurs only after a sustained loss in calcium homeostasis. Processing of NCX3 or other calpain substrates is unlikely to be the primary cause of acute excitotoxicity in cortical neurons. However, a role for calpain as a contributing factor or in response to milder glutamate insults is not excluded.

Keywords: apoptosis, calpeptin, excitotoxicity, necrosis, NMDA, sodium-calcium exchanger.

J. Neurochem. (2009) **110**, 990–1004.

Modes of cell death in acute and chronic neurodegenerative disorders are widely varied and brain-region selective pathology is frequently observed (Bredesen *et al.* 2006; Lin and Beal 2006). Despite this variability there is a pervasive view that antagonizing Ca²⁺-dependent calpain proteases is universally protective. Two ubiquitous isoforms, μ-calpain (EC 3.4.22.52) and m-calpain (EC 3.4.22.53), are implicated in neurodegeneration (Bever and Neumar 2008). *In vitro*, these isoforms are activated by micromolar and millimolar concentrations of calcium, respectively. Although intracellular calcium in healthy neurons is generally ~100 nM and does not reach millimolar levels until complete loss of calcium homeostasis occurs (Randall and Thayer 1992; Nicholls 2004), calpain activation prior to calcium deregulation has been explained by proximity to NMDA receptors (Adamec *et al.* 1998; Hewitt *et al.* 1998; Vanderklis *et al.* 2000), sodium-calcium exchangers (NCX) (Araujo *et al.* 2007), or other routes of local calcium elevation (Friedrich 2004).

Received March 20, 2009; revised manuscript received May 20, 2009; accepted May 20, 2009.

Address correspondence and reprint requests to Brian M. Polster, Department of Anesthesiology, University of Maryland School of Medicine, 685 W. Baltimore St, MSTF 5-34, Baltimore, MD 21201, USA. E-mail: bpolster@anes.umm.edu or Akos A. Gerencser, Buck Institute for Age Research, 8001 Redwood Blvd., Novato, CA 94945, USA. E-mail: agerencser@buckinstitute.org

¹Both these authors contributed equally to this study.

Abbreviations used: ΔΨ_p, plasma membrane potential; AM, acetoxymethyl ester; AMPA, α-amino-3-hydroxy-5-methylisoxazole-4-propionate; CFP, cyan fluorescent protein; DCD, delayed calcium deregulation; DIV, days *in vitro*; eYFP, enhanced yellow fluorescent protein; FRET, fluorescence resonance energy transfer; GluR, glutamate receptor; NBQX, 2,3-dihydroxy-6-nitro-7-sulfamoyl-benzo[f]quinoxaline-2,3-dione; NCX, sodium-calcium exchanger; ND, neutral density; PI, propidium iodide; PMPI, plasma membrane potential indicator; RCE, reversible calcium elevations; SDS, sodium dodecyl sulfate; TMRM⁺, tetramethylrhodamine methyl ester; YFP, yellow fluorescent protein.

Calpain activation near glutamate receptors (GluR) was reported within 5 min of NMDA receptor activation (Lankiewicz *et al.* 2000; Vanderklish *et al.* 2000). NMDA, α -amino-3-hydroxy-5-methylisoxazole-4-propionate (AMPA), and metabotropic GluR1 receptor subunits are initial targets of calpain processing (Guttmann *et al.* 2002; Simpkins *et al.* 2003; Wu *et al.* 2005; Xu *et al.* 2007; Yuen *et al.* 2007a,b). By ameliorating the extent of intracellular Ca^{2+} and Na^{+} elevation during short bursts of GluR over-activation, these initial proteolysis events may protect the neuron from 'accidental excitotoxicity.' In contrast, sustained GluR activation leads to the calpain-dependent processing of numerous substrates, many with deleterious consequences for cell survival. Substrates include the cytoskeletal proteins α -spectrin and microtubule-associated protein 2 (Siman and Noszek 1988; Springer *et al.* 1997), plasma membrane calcium ATPases (Pottorf *et al.* 2006), calcineurin phosphatase (Wu *et al.* 2004), the cyclin-dependent kinase 5 activator p35 (Lee *et al.* 2000), and apoptosis-inducing factor (Polster *et al.* 2005; Cao *et al.* 2007).

The point-of-no-return for a neuron succumbing to excitotoxic injury is generally considered the time at which intracellular calcium homeostasis is irreversibly lost, i.e. delayed calcium deregulation (DCD) (Nicholls 2004). Events that contribute to the onset of DCD are predicted to influence cell survival with an opportunity for therapeutic intervention. However, events that occur after DCD are predicted to influence the timing of cell death without altering its inevitability. Calpain processing of NCX isoform 3 and loss of calcium extrusion capacity was directly implicated in the delayed calcium rise observed in glutamate-treated cerebellar granule neurons (Bano *et al.* 2005). However, the expression of cleavage-resistant NCX1 as compared to NCX3 is higher in forebrain neurons when compared with cerebellar granule neurons (Kiedrowski *et al.* 2004) although granule neurons are more resistant to DCD (Brorson *et al.* 1995; Castilho *et al.* 1998; Stout *et al.* 1998; Vergun *et al.* 1999; Bano *et al.* 2005; Bolshakov *et al.* 2008). This raises the possibility that alternate mechanisms precipitate DCD in forebrain neurons before calpain-mediated loss of functional NCX3 limits calcium homeostasis.

In this study, we tested the hypotheses that (i) DCD can occur without calpain activation in primary cortical neurons exposed to an excitotoxic concentration of glutamate and (ii) calpain activation converts DCD from a reversible to an irreversible event. This was accomplished by conducting simultaneous live cell imaging of calpain activation and intracellular calcium deregulation, investigating the function and processing of NCX, and testing the efficacy of calpain inhibitors against DCD, DCD-like reversible calcium elevations (RCE), and cell death. Our results define major cytoplasmic calpain activation in forebrain neurons as a distinct event occurring downstream of DCD that is not required for acute glutamate toxicity.

Materials and methods

Materials

Tetramethylrhodamine methyl ester (TMRM⁺), Fura-4F-acetoxymethyl ester (AM), Fura-6F-AM, Fluo-4FF-AM, SBFI-AM, lipofectamine 2000, Neurobasal medium, B27 supplement, and GlutaMAX were from Invitrogen (Carlsbad, CA, USA). Ionomycin, calpeptin, and PD150606 were purchased from EMD Biosciences (San Diego, CA, USA). Primary rabbit polyclonal antibody to NCX3 was a kind gift of Dr Ken Philipson (UCLA, Los Angeles, CA, USA). Mouse monoclonal antibody to β -actin (clone AC-74) was from Sigma (St Louis, MO, USA). Mouse monoclonal antibody to α -spectrin (MAB1622) was from Chemicon (Temecula, CA, USA). The pYSCS plasmid was generously provided by Dr Peter Vanderklish (The Scripps Research Institute, San Diego, CA, USA). All other reagents were purchased from Sigma unless otherwise indicated.

Preparation of primary neurons

Primary cortical neurons were prepared from 1 to 2 pairs of embryonic day 18 rat cortices (BrainBits™; LLC, Springfield, IL, USA) by papain dissociation followed by gentle trituration and used at 11–14 days *in vitro* (DIV). Briefly, cortices were washed in 2 mL of Hibernate™ medium (BrainBits™) and then digested with 2 mg/mL papain (Worthington, Lakewood, NJ, USA) in Hibernate™ for 30 min at 37°C. Tissue was dispersed manually by 5–10 strokes with a 1 mL pipette and cells were plated onto poly-D-lysine-coated Lab-Tek eight-well chambered cover glasses (Nunc, Naperville, IL, USA) at a density of 1×10^5 cells/well. Cells were initially plated in Neurobasal medium containing B27 supplement (2%), L-glutamine (0.5 mM), fetal bovine serum (1%), penicillin (100 IU/mL), and streptomycin (100 μ g/mL). For the majority of experiments, neurons were maintained at 37°C in an oxygen-regulated incubator with a humidified atmosphere of 92% N₂/5% CO₂/3% O₂. Every 3–4 days after the initial plating, half of the medium was replaced with fresh medium lacking serum and containing GlutaMAX (0.5 mM) in place of L-glutamine. When stated, results with neurons cultured at physiologically relevant 3% O₂ (Grote *et al.* 1996) were confirmed using neurons cultured in a conventional 95% air/5% CO₂ environment. All experiments were conducted in room air.

Wide-field functional imaging

For simultaneous assay of DCD and calpain activation, cortical cultures were transfected with the pYSCS fluorescence resonance energy transfer (FRET) sensor (Vanderklish *et al.* 2000) on day 9 using Lipofectamine 2000 (Invitrogen) in Neurobasal medium at a 3 : 2 ratio of Lipofectamine (μ L) to DNA (μ g); 0.2 μ g of DNA was transfected per well in eight-well Lab-Tek chambers. Experiments were carried out at 3 days post-transfection (at 12 DIV). The pYSCS-transfected cultures were incubated with Fura-6F-AM (3 μ M) for 25 min at 37°C in imaging medium containing (in mM): 120 NaCl, 3.5 KCl, 1.3 CaCl₂, 0.4 KH₂PO₄, 20 N-Tris-(hydroxymethyl)-methyl-2-amino-ethanesulfonic acid, 5 NaHCO₃, 1.2 Na₂SO₄, 15 D-glucose, and the pH was set to 7.4 by NaOH [considering a pK_a of 7.5 for N-Tris-(hydroxymethyl)-methyl-2-amino-ethanesulfonic acid, by 8.9 mM NaOH, yielding $[\text{Na}^+]_e = 136\text{mM}$]. For dye loading or in experiments with superfusion, the imaging medium was supplemented with MgCl₂ (1 mM).

To image initial glutamate-triggered ionic changes, untransfected cortical cultures were incubated with Fura-4F-AM (1 μM) for 20 min or with SBFI-AM (6 μM ; in the presence of 0.02% Pluronic F127) for 40 min at 37°C in Mg^{2+} -supplemented imaging medium and subsequently rinsed. To monitor plasma membrane potential ($\Delta\Psi_p$), the plasma membrane potential indicator [PMPI; Molecular Devices (Sunnyvale, CA, USA) #R8042 FLIPR Membrane Potential Assay Kit] was used at 1 : 200 dilution of the *Loading Buffer* (specified by the manufacturer).

Imaging was performed on an Olympus IX-81 inverted microscope (Olympus, Center Valley, PA, USA) equipped with a UAPO™ 20 \times air 0.75 NA lens, a Lambda LS Xe-arc light source (175 W), Lambda 10-2 excitation and emission filter wheels (Sutter Instruments, Novato, CA, USA), a ProScan linear-encoded *xy*-stage (Prior, Rockland, MA, USA) and a Coolsnap HQ cooled digital charge coupled device camera (Photometrics, Tucson, AZ, USA). The filter sets given as excitation-dichroic mirror-emission (in nm) were: for yellow fluorescent protein (YFP) or PMPI 500/24 (band pass) – 520LP (long pass) – 542/27 (Semrock, Rochester, NY, USA); for cyan fluorescent protein (CFP) 438/24 – 458LP – 483/32 (Semrock); for FRET 438/24 – 458LP – 542/27 (Semrock); and for Fura dyes and SBFI 340 or 380 (Chroma, Rockingham, VT, USA) – 458LP – 420LP. The whole microscope was maintained at 37°C in air using an environmental enclosure.

Measurement of the kinetics of calpain activation and DCD

Image acquisition was controlled by the Multi-Dimensional Acquisition application in METAMORPH 6.3 (Molecular Devices). Images were recorded by using a neutral density (ND) 1.0 attenuator, 100–200 ms exposure times and 3 \times 3 binning in 2-min intervals in 12 view fields at the following five wavelengths (defined above): YFP, CFP, FRET, Fura 340, and Fura 380 nm. In each acquisition cycle, the sample was auto-focused on green fluorescent beads placed in an empty well of the eight-well chamber. Fluorescence intensities were determined over the soma of pYSCS-expressing neurons after background subtraction. The background was defined by the peak of the intensity histogram of each frame. All of the following calculations were performed by the region of interest average intensities, except for images and movies shown, where calculations were performed pixel-by-pixel.

The FRET probe pYSCS responds to the proteolysis of its α -spectrin calpain cleavage site with an irreversible loss of FRET (Vanderklish *et al.* 2000). Although a portion of the encoded protein localized to post-synaptic densities, the majority of the fluorescence was in the cytoplasm. We found that the fluorescence of the YFP component of pYSCS exhibited a substantial decrease in intensity when neurons were stimulated with glutamate or underwent DCD. This observation is consistent with quenching of the eYFP FRET acceptor by a decrease in pH or an increase of $[\text{Cl}^-]$ in glutamate-stimulated neurons (Wu *et al.* 1999; Zhang *et al.* 2002; Slemmer *et al.* 2004). In addition to the crosstalk between CFP, YFP, and FRET channels, fluorescence of Fura-6F significantly contributed to the CFP and FRET images and the CFP and the YFP to the Fura-6F emission in brightly expressing cells. Therefore, the measured fluorescence intensities (F) were first spectrally (linearly) unmixed (resulting fluorescence intensities specific for each fluorophore F' ; see Supporting Materials and methods). $[\text{Ca}^{2+}]_c$ is given as the ratio of unmixed Fura-6F intensities ($R_{\text{Fura6F}} = F'_{340}/F'_{380}$). Because of

saturation concentrations of intracellular calcium after DCD R_{Fura6F} was not calibrated to show micromolarity. To correct for the loss of eYFP fluorescence yield, a three wavelength-corrected FRET ratio calculation was used in place of a simple emission ratio that was used earlier in fixed cells, where ionic effects did not contribute (Vanderklish *et al.* 2000). This was expressed as $\text{FRET} = F'_{\text{FRET}}/\sqrt{F'_{\text{CFP}}F'_{\text{YFP}}}$. Image analysis was performed in custom software developed in Delphi 2009 (Embarcadero Technologies, San Francisco, CA, USA).

Cross-correlation analysis

The kinetics of corrected FRET ratio and Fura-6F ratio were heterogeneous among neurons. To provide a relative comparison of changes in these signals, temporal cross-correlation of differentiated signals was calculated. Because cross-correlograms show the relative relationship of compared signals in time, the cell-by-cell heterogeneity cancels and the mean of the correlograms can be calculated. Calculations were performed using standard functions of MATHEMATICA 5.2 (Wolfram Research, Champaign, IL, USA) (Appendix S1). Cross-correlograms provide the following information when ‘trace 1’ (FRET) is compared with ‘trace 2’ (Fura-6F): changes in traces 1 and 2 occurring at the same time in the same direction (increase or decrease) are indicated by a positive peak at zero time. Changes occurring at the same time in the opposite direction (for instance decrease in 1 and increase in 2) are indicated by a negative peak. When the change in 1 occurs after the change in 2, the peak of the cross-correlation diagram shifts to a positive time lag.

Initial changes of ion concentrations during glutamate exposure

Wide-field image acquisition was performed as stated above, but by METAFUOR 6.3 (Molecular Devices). For imaging Fura-4F, an ND 1.5 attenuator, 4 \times 4 binning, and 400 and 200 ms exposure times were used for the 340 and 380 nm excitations, respectively, at a 4 s image acquisition interval. For imaging SBFI plus PMPI, an ND 0.5 attenuator, 4 \times 4 binning, and 300, 100, and 30 ms exposure times were used for SBFI 340, 380 nm and PMPI 500 nm excitations, respectively. There was no measurable crosstalk between SBFI and PMPI emissions.

Fura-4F ratios ($R = F_{340}/F_{380}$) were calibrated to micromolarity using the $[\text{Ca}^{2+}] = K_d \times [(R - R_{\text{min}})/(R_{\text{max}} - R)] \times F_{\text{free380}}/F_{\text{sat380}}$ equation (Grynkiewicz *et al.* 1985). Cells were exposed to zero and saturating (10 mM free) $[\text{Ca}^{2+}]$, yielding the minimal fluorescence ratio (R_{min}) plus the intensity of the Ca^{2+} -unbound Fura-4F at the 380 nm excitation (F_{free380}) and the maximal ratio (R_{max}) plus the intensity of Ca^{2+} -saturated Fura-4F at the 380 nm excitation (F_{sat380}), respectively. To calculate the $F_{\text{free380}}/F_{\text{sat380}}$ ratio, cell swelling and dye leakage were compensated by normalization of F_{free380} and F_{sat380} with the isosbestic fluorescence intensity calculated for the matching time points (Gerencser and Nicholls 2008). To obtain the above parameters, the imaging medium was replaced with ‘intracellular medium’ containing (in mM): 123 KCl, 12.4 NaCl, 20 KOH, 10 EGTA, 20 PIPES with, and then, without 20 mM CaCl_2 , pH 7.2, and supplemented with 20 μM 4Br-A23187 (AG Scientific, San Diego, CA, USA), 10 μM nigericin, 10 μM monensin, and 1 μM antimycin A to establish complete equilibration of $[\text{Ca}^{2+}]$ and pH (Gerencser and Adam-Vizi 2005). The K_d of Fura-4F was taken as 770 nM according to the manufacturer. SBFI

was calibrated similarly to Fura-4F, but parameters were obtained by a three-point calibration at rest (where $[Na^+]_c$ was 11.4 ± 0.3 mM; $n = 3$; determined in separate experiments), after complete equilibration with the imaging medium ($[Na^+]_e = 136$ mM) in the presence of gramicidin ($10 \mu\text{g/mL}$), and after wash with nominally Na^+ -free (choline chloride substituted) medium. This calibration provided R_{min} , R_{max} , and $K_d \times F_{free380}/F_{sat380}$ from ratios measured at the above conditions (see Supporting Materials and methods). The PMPI fluorescence was converted to millivolts by a dynamic, Nernstian, compartment model-based calibration technique (see Supporting Materials and methods). The calibration was based on the measurement of PMPI fluorescence at K^+ -equilibrium potential (-80.4 mV) in the presence of valinomycin ($1 \mu\text{M}$; a K^+ -selective ionophore) and oligomycin ($2 \mu\text{g/mL}$) (at $[K^+]_e = 3.9$ mM and $[K^+]_c = 79.1 \pm 1.4$ mM; $n = 3$), and at zero $\Delta\Psi_p$ after addition of gramicidin ($10 \mu\text{g/mL}$; a K^+ - Na^+ -ionophore). The resting $\Delta\Psi_p$ was -59.9 ± 1.2 mV ($n = 3$ experiments). For the glutamate-treatment experiments, the resting and zero potentials were used as calibration points, and the gramicidin treatment was the common calibration step with the $[Na^+] = 136$ mM point of the SBFI calibration. This procedure was performed at the end of each experiment and calculations were performed cell-by-cell in MATHEMATICA 5.2. The mean \pm SE of the calibrated values are shown.

Calculation of the Gibbs-free energy (ΔG) of the NCX

To calculate ΔG , the measured mean $[Ca^{2+}]_c$, $[Na^+]_c$, and $\Delta\Psi_p$ in addition to $[Na^+]_e = 136$ mM and $[Ca^{2+}]_e = 1.3$ mM were used:

$$\Delta G = RT \log \frac{[Ca^{2+}]_e [Na^+]_c^n}{[Ca^{2+}]_c [Na^+]_e^n} + (2 - n)F\Delta\Psi_p \quad (1)$$

In eqn. 1, $R = 8.3$ J/mol/K (gas constant), $T = 310$ K (temperature), $F = 96485$ J/mol/V (Faraday constant), n is the exchange ratio, and the $\Delta\Psi_p$ is given in negative volts. The exchange ratio of $Na^+ : Ca^{2+}$ is known to be near to 3 : 1, but higher, non-integer values were also often reported (Blaustein and Lederer 1999; Bers and Ginsburg 2007). In resting neurons, the NCX is considered to be in equilibrium, thus its ΔG is zero. In our case, this was satisfied with $n = 3.1$, therefore this value was used to calculate ΔG . The error of ΔG was calculated by propagating the SE of the measured parameters though the calculations (Gerencser *et al.* 2008).

Imaging the time-course of DCD, membrane potential changes, and cell death

Imaging was performed using an LSM™ 5 Pascal laser scanning confocal system (Carl Zeiss AG, Oberkochen, Germany) with a 20× NEOFLUAR NA 0.5 air objective lens in room air in a temperature-controlled enclosure at 37°C. For simultaneous imaging of DCD and membrane potential changes, neurons in eight-well Lab-Tek chambers were loaded with Fluo-4FF-AM ($0.5 \mu\text{M}$) and TMRM⁺ (5 nM) in the presence of tetraphenylboron ($1 \mu\text{M}$) in imaging medium for 60–90 min at 37°C. Fluo-4FF and TMRM⁺ were simultaneously excited at 488 and 543 nm and emissions were monitored using 505–530 nm and a 560LP filter, respectively. There was no measurable crosstalk between the emissions of Fluo-4FF and TMRM⁺.

Fluorescent time-courses from four independent wells of the Lab-Tek dish were acquired in parallel using the Multi-Time Lapse Module, recording a time point for each well at every 4 min.

Neurons displaying TMRM⁺ fluorescence that was lost upon glutamate stimulation (signifying $\Delta\Psi_p$ depolarization) were selected for analysis.

For cell viability experiments, membrane potential polarization, apoptosis, and cell death were determined in parallel using TMRM⁺, the early plasma membrane permeabilization marker Yo-Pro-1, and the necrosis marker propidium iodide (PI), respectively. The dyes were simultaneously excited at 488 and 543 nm, and emissions were detected at 505–530 nm for Yo-Pro-1, at 560–615 nm for TMRM⁺ and at 608–683 nm for PI. The PI staining was punctate and distinctly nuclear while TMRM⁺ fluorescence was cytoplasmic, enabling us to use these dyes in concert despite partial spectral overlap. Neurons pre-treated with $10 \mu\text{M}$ calpeptin or vehicle for 30 min in imaging buffer were subsequently exposed to glutamate. After 30 min of glutamate or vehicle treatment, imaging buffer was removed and replaced with previously saved culture medium diluted with fresh medium at 1 : 1. This medium was supplemented with HEPES (20 mM) to buffer pH and MK801 ($10 \mu\text{M}$) and 2,3-dihydroxy-6-nitro-7-sulfamoyl-benzof[*f*]quinoxaline-2,3-dione (NBQX; $10 \mu\text{M}$) to block NMDA and AMPA receptors, respectively. The number of healthy neurons defined as TMRM⁺ positive, PI negative, the number of apoptotic neurons defined as Yo-Pro-1 positive, PI negative, and the number of necrotic neurons defined by PI positive nuclear staining were counted at 0, 4, 8, 12, and 20 h following glutamate treatment.

Immunoblot analysis

Following the acquisition of fluorescent time-courses, imaging buffer was aspirated from the wells and neurons were lysed by scraping in 50 μL of radioimmunoprecipitation assay buffer consisting of 150 mM NaCl, 50 mM Tris, 1 mM EDTA, 1 mM EGTA, 1% Triton X-100, 0.5% sodium deoxycholate, 0.1% sodium dodecyl sulfate (SDS), and 1x Halt Protease Inhibitor Cocktail (Pierce Biotechnology, Rockford, IL, USA) or Protease Inhibitor Cocktail Set III (EMD Biosciences), pH 7.4. Solubilization of membrane proteins was enhanced by three freeze–thaw cycles followed by incubation in SDS–polyacrylamide gel electrophoresis sample buffer containing 5% β -mercaptoethanol for 30 min at 37°C. Seven to 20 μg of neuronal protein was separated on 4–20% Tris–HEPES gradient gels (ISC BioExpress, Kaysville, UT, USA) by SDS–polyacrylamide gel electrophoresis and transferred to polyvinylidene difluoride membranes (Bio-Rad, Hercules, CA, USA). Immunodetection was performed by standard procedures using SuperSignal West Pico or West Femto enhanced chemiluminescence substrates (Pierce Biotechnology) and the following dilutions of primary antibodies: 1 : 500 anti- α -spectrin ($0.2 \mu\text{g/mL}$), 1 : 5000 anti- β -actin, 1 : 1000 anti-NCX3.

Statistical analysis

The incidence and time to DCD in the absence and presence of calpain inhibitor was analyzed for statistical differences using paired Student's *t*-test comparing the same-day controls. Numbers of neurons exhibiting RCE or recovery were compared with Fisher's exact test in GRAPHPAD Prism 4 (GraphPad Software, Inc., San Diego, CA, USA). To examine whether calpeptin modified the effect of glutamate on TMRM⁺ or PI fluorescence, logistic regression analysis was used (see Supporting Materials and methods). Averages are represented in the text as mean \pm SE.

Results

Real-time visualization of calpain activation and DCD

Cytoplasmic calcium changes and calpain activity were monitored in single cells simultaneously with wide-field microscopy using the low affinity Ca^{2+} dye Fura-6F (Fig. 1a) and the FRET-based, genetically encoded calpain sensor pYSCS (Fig. 1b), respectively. Cleavage of the pYSCS-encoded protein within the α -spectrin sequence targeted by calpain is expected to trigger an irreversible loss of the FRET between the CFP FRET donor and the YFP FRET acceptor (Vanderklish *et al.* 2000). Cortical cultures were pre-treated with calpeptin (10 μM) or vehicle (dimethylsulfoxide 1 : 2000) for 30 min and then exposed to glutamate (100 μM ; with 10 μM glycine in the absence of Mg^{2+}). Calpeptin (or vehicle) and glutamate were present for the duration of the experiment.

Glutamate evoked a small initial increase in intracellular calcium, as monitored by the Fura-6F ratio over the soma (Fig. 1c–d, black trace, Movie S1). This small calcium increase was followed by DCD at 5–30 min [red pseudocolor in Fig. 1a (ii and iii)]. The initial response of the calpain sensor to glutamate was a $14.1 \pm 0.8\%$ drop in the amount of FRET in the soma (compared with the baseline; $n = 58$, Fig. 1c, red trace) that was not inhibited by calpeptin ($15.2 \pm 0.9\%$ $n = 59$). Moreover, in the presence of calpeptin, this initial decrease in FRET spontaneously reversed, excluding the possibility that this drop was due to irreversible cleavage of the sensor by calpain [Fig. 1d, red trace and b(ii)]. Shortly before DCD the FRET exhibited another calpeptin-insensitive and reversible decrease (Fig. 1c and d, open arrows). The only *calpeptin-sensitive*, irreversible, ‘major drop of FRET’ (to $37 \pm 3\%$ below baseline; $n = 23$) likely to reflect calpain activation occurred long after DCD [Fig. 1c, red arrow and b(iii) cells B and C, Movie S2]. Forty-four of the 58 vehicle pre-treated cells underwent DCD (at 20 ± 3 min after addition of glutamate), and 23 of these also exhibited ‘calpain activation’ typical to that denoted by the red arrow in Fig. 1c. No such change in FRET occurred in cells that did not undergo DCD. We observed only two cells with similar FRET characteristics in 49 calpeptin pre-treated neurons undergoing DCD.

Pairs of boxes in Fig. 1e depict the time to DCD and the time to ‘calpain activation’ (relative to glutamate addition) for individual neurons. Pairs connected by lines with a positive (upward) slope indicate neurons exhibiting ‘calpain activation’ subsequent to DCD. Of note, ‘calpain activation’ was objectively defined as the steepest decrease in FRET beyond a threshold using a computer algorithm. In a few cells (negatively sloped lines in Fig. 1e), the small second drop (Fig. 1c and d, open arrows) was categorized as ‘calpain activation’ by the criterion of steepest decrease. Cells that exhibited DCD but no ‘calpain activation’ during the

measured time frame are shown by triangles. The mean lag time between DCD and calpain activation was 39 ± 5 min ($n = 23$).

The relationship between DCD (increase in Fura-6F ratio) and calpain activation (decrease in pYSCS FRET) was also quantified by calculation of temporal cross-correlation of differentiated signals (Fig. 1f and g). The only marked change in the Fura-6F ratio in the 5–120 min time window after glutamate addition was the increase corresponding to DCD. In contrast the FRET signal typically exhibited multiple drops. In the cross-correlograms (Fig. 1f and g), negative peaks mark changes in the two signals in opposite directions (see Materials and methods). Both control and calpeptin-treated cross-correlograms (Fig. 1f and g) indicate a drop of the FRET signal shortly before DCD (open arrows) that corresponds to the reversible, calpeptin-insensitive decrease in FRET. Importantly, the mean cross-correlogram in vehicle control-treated neurons (Fig. 1f, solid arrow) has a second negative peak at +39 min that is not present in calpeptin pre-treated cells (Fig. 1g). This calpeptin-sensitive negative peak indicates the occurrence of calpain activation at an average of 39 min after DCD, confirming the ‘binary’ calculations of Fig. 1e. The incidence and onset of DCD in pYSCS-transfected neurons was not significantly different in calpeptin-treated cultures; 49 of 59 neurons pre-treated with calpeptin underwent DCD (at 15 ± 3 min, $n = 49$) compared with 44 of 58 (at 20 ± 3 min, $n = 44$) pre-treated with the vehicle control.

A possible spatial heterogeneity of glutamate-triggered calpain activation was also investigated in FRET images [Fig. 1b(i–iii)]. Detectable calpain activation (defined as the ‘major drop of FRET’) occurred after dendrites formed injury-related varicosities [Fig. 1b(ii)], and happened simultaneously in the soma and along the dendrites [e.g. Fig. 1b(iii) and Movie S2]. However, the possibility of an earlier, local activation of calpain prior to DCD cannot be fully excluded by using pYSCS, because of the large calpeptin-insensitive changes as well as the small true FRET signal compared with the noise amplified by the spectral and FRET corrections.

Our imaging experiments were conducted with neurons cultured for 11–14 DIV at 3% O_2 , physiologically relevant to the average 2–4% O_2 (15–30 mm Torr) that was measured in the rat cortex (Grote *et al.* 1996). Because much of the literature on glutamate excitotoxicity investigates neurons cultured at 95% air/5% CO_2 (~20% O_2), we repeated the Fura-6F pYSCS imaging experiments on cortical cultures grown in parallel at 20% O_2 . A slightly higher incidence of DCD during the measurement period was observed in neurons grown at 20% O_2 (37 deregulating neurons of 39 total cells) compared with those grown at 3% O_2 (44 of 58). However, the properties of calpain activation were almost identical, with 18 of the 37 deregulating neurons showing calpain activation with a 46 ± 4 min delay. None of the 20% O_2 -cultured neurons pre-treated with calpeptin displayed the

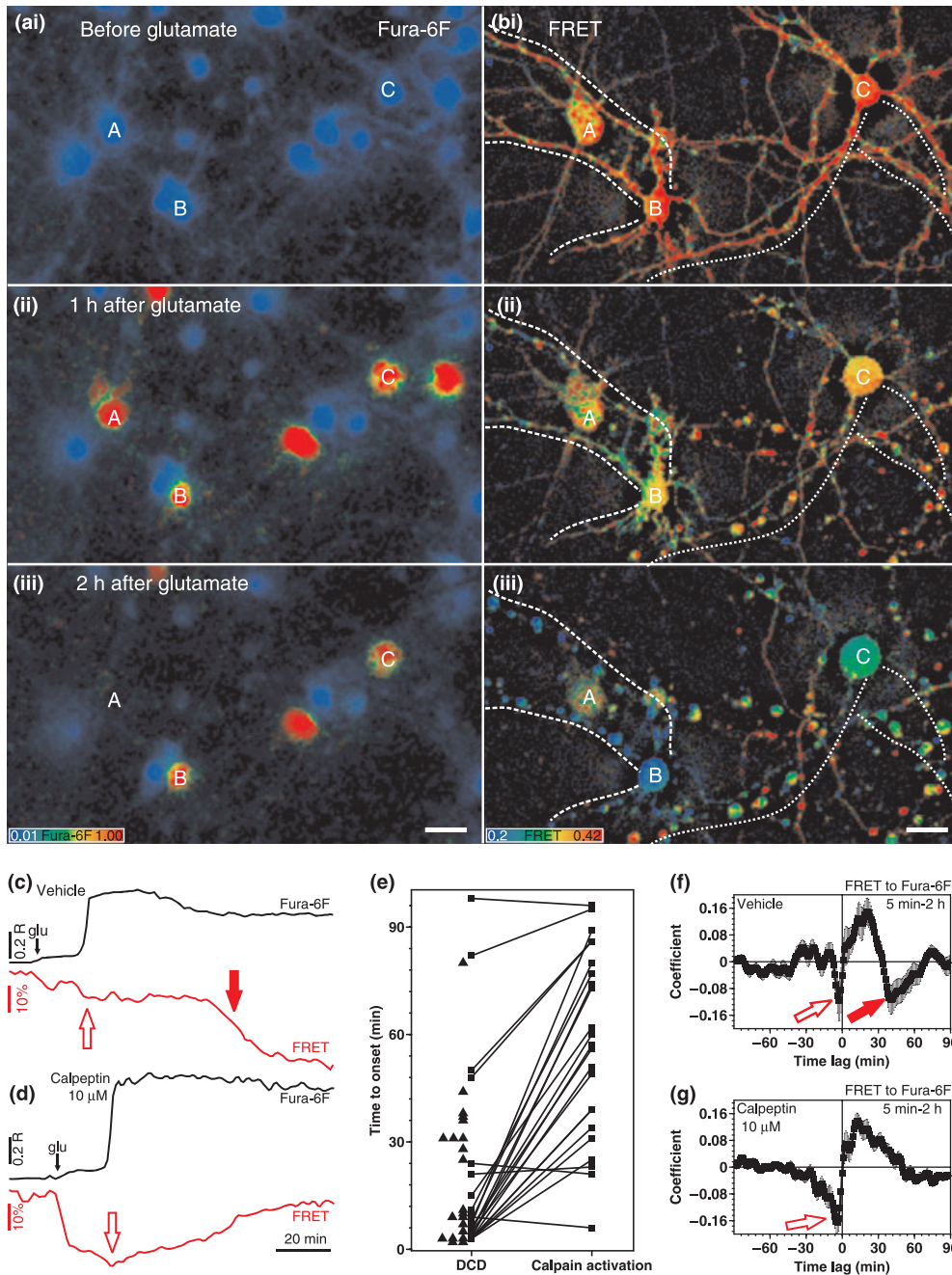


Fig. 1 The temporal relationship of DCD and calpain activation. Cortical cultures expressing the calpain sensor pYSCS were wide-field time lapse imaged during continuous exposure to glutamate. (a) Fura-6F pseudo-colored ratio images. Cells A–C identify three cells expressing pYSCS in (b). Cells not appearing in [a(iii); e.g. cell A] underwent lysis. (b) Spectrally unmixed, aligned, corrected pYSCS FRET ratio images gated with the deheized (high pass filtered) YFP acceptor fluorescence image. Dashed and dotted lines follow dendrites of cells B and C, respectively. Scale bars, 20 μ m. (c–d) Representative pairs of Fura-6F ratio (R; black) and corrected FRET ratio (% of baseline; red) traces from a vehicle (c) and a calpeptin (d; 10 μ M, 30 min) pre-treated neuron. Open red arrows indicate a DCD-related, but calpeptin-insensitive decrease in FRET. The solid red

arrow in (c) indicates the ‘major drop of FRET’ associated with calpain activation. (e) Onset times of DCD and calpain activation as compared with the application of glutamate. Boxes connected with lines indicate individual neurons exhibiting both DCD and calpain activation. Triangles indicate neurons with DCD but no calpain activation. (f) Mean \pm SE of temporal cross-correlatograms comparing changes in FRET ratio to Fura-6F ratio. Data indicate mean \pm SE of the cross-correlation diagrams calculated for neurons showing calpain activation in the vehicle-treated condition (f, $n = 23$), and for neurons exhibiting DCD in the calpeptin-treated condition (g, $n = 49$). Red arrows correspond to arrows in (c–d). Data were pooled from experiments using five different cell culture batches.

Treatment (μM)	% O ₂ of culture	% DCD at 20 min	% DCD at 60 min	Number of cells	Number of view fields
Calpeptin (10)	3	109.9 \pm 6.7*	115 \pm 6.4*	705	27
PD150606 (10)	3	68.2 \pm 14.0	83.1 \pm 8.4	384	6
PD150606 (50)	3	11.8 \pm 4.8*	44.7 \pm 11.8*	300	6
KB-R7943 (10)	3	31.4 \pm 10.7*	57.6 \pm 11.7*	348	6
Calpeptin (10)	20	125.7 \pm 10.6*	112.2 \pm 4.3*	590	18
PD150606 (10)	20	71.8 \pm 7.1*	92.0 \pm 6.2	303	6
PD150606 (50)	20	17.0 \pm 3.4*	41.0 \pm 6.1*	302	5
KB-R7943 (10)	20	56.1 \pm 9.4*	77.8 \pm 10.9	312	6

Table 1 Incidence of glutamate-induced DCD in the presence of calpain or NCX inhibitors relative to same-day controls

Nifedipine (1 μM) was present in experiments with KB-R7943 and in the corresponding controls to exclude the possibility that action was due to effects on voltage-dependent Ca²⁺ channels. Significance was determined by comparing the relative incidence of DCD in *n* view fields to 100% using a two-tailed Student's *t*-test; **p* < 0.05.

secondary loss of FRET that we associated with calpain activation.

To exclude the possibility that the calpain FRET sensor either influenced the onset of DCD or occluded an effect of calpeptin on DCD onset, we also quantified DCD in the untransfected cell population for the same experiments. As with pYSCS-transfected neurons, calpeptin did not delay the onset of DCD. In contrast, after analyzing a large number of cells we detected a slight but significant increase in the incidence of DCD following 60 min of glutamate exposure in calpeptin-treated neurons (Table 1). Similar results were obtained with neurons cultured at 20% O₂.

Independent evaluation of the effect of calpeptin on DCD and calpain inhibition

To additionally confirm that calpeptin does not inhibit DCD, we imaged DCD using a different low affinity calcium indicator (Fluo-4FF; *K_d* \sim 9.7 μM) in conjunction with the membrane potential sensitive dye TMRM⁺. Fluo-4FF undergoes a marked increase in fluorescence once calcium homeostasis is lost (Fig 2b, arrows) but is relatively insensitive to calcium increases (\sim 1 μM) mediated by the NMDA receptor (Fig. 2b, arrowhead) (Vesce *et al.* 2004). Prior to glutamate addition, neurons displayed little Fluo-4FF fluorescence and a mitochondrial pattern of TMRM⁺ fluorescence, indicative of healthy cells with polarized plasma and mitochondrial membrane potentials (Fig 2a). Following glutamate addition, TMRM⁺ fluorescence was lost and neurons exhibited a stochastic and dramatic rise in Fluo-4FF fluorescence (Fig 2b and c). Under our conditions where the concentration of TMRM⁺ is insufficient to result in mitochondrial matrix quenching, the drop of TMRM⁺ signal in response to glutamate primarily reflects $\Delta\Psi_P$ depolarization (Nicholls 2006) and was used to unambiguously identify neurons responding to glutamate.

Primary cortical neurons lost calcium homeostasis following 100 μM glutamate exposure with a DCD incidence and

onset that was not significantly different in the absence or presence of calpeptin; 109 of 110 neurons pre-treated with calpeptin underwent DCD by 60 min (at 18 \pm 4 min; *n* = 4) compared with 106 of 107 pre-treated with the vehicle control (at 15 \pm 2 min; *n* = 4). Intracellular calcium responses in individual cells (Fig. 2c–d) and averaged Fluo-4FF responses (Fig. 2e) from a representative experiment are depicted in Fig. 2. In some experiments, the calcium ionophore ionomycin (5 μM) was added after the large Fluo-4FF increase associated with DCD. Neurons displaying high Fluo-4FF fluorescence demonstrated no further increase upon ionomycin addition, confirming that DCD had occurred in these cells.

Analysis of α -spectrin and NCX3 cleavage in glutamate-treated cortical neurons

While the calpain FRET sensor experiments suggested that calpeptin was an effective calpain inhibitor, it was important to obtain independent confirmation of intracellular calpain activation and the efficacy of calpain inhibition in our paradigm. Therefore, cortical neurons incubated with glutamate for 1.5 h in the presence and absence of calpeptin were harvested following calcium imaging and subjected to immunoblot analysis for the canonical calpain substrate α -spectrin. Consistent with the proteolysis of the α -spectrin-based calpain FRET sensor, we observed glutamate-induced processing of α -spectrin that was inhibited by calpeptin (Fig. 3). Densitometry indicated that calpeptin inhibited the appearance of the α -spectrin breakdown product by > 90%. Thus, calpeptin was an effective inhibitor of calpain activation in our experiments even though it was not an effective inhibitor of DCD.

In contrast to α -spectrin, a decrease in full-length NCX3 was not observed (Fig. 3). The 58–60 kDa cleavage products reported in glutamate-treated cerebellar granule neurons (Bano *et al.* 2005) were barely detectable in cortical neurons relative to full-length NCX3 following 1.5 h of glutamate

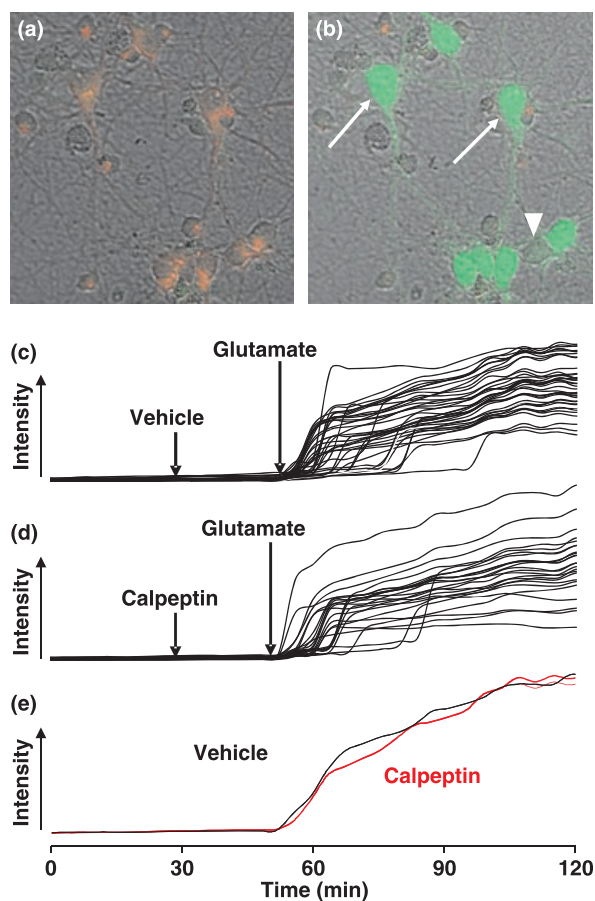


Fig. 2 The effect of calpeptin on DCD in neurons imaged with Fluo-4FF. Neurons loaded with the membrane potential sensitive dye TMRM⁺ (red) and the calcium indicator Fluo-4FF (green) are depicted before (a) and 16 min after (b) treatment with 100 μM glutamate. Arrows identify examples of cells with intense Fluo-4FF fluorescence that underwent calcium deregulation while the arrowhead denotes a cell that did not yet exhibit DCD although it depolarized in response to glutamate. In (c–d), Fluo-4FF responses in individual cells from representative fields of neurons are plotted over time in the absence (c) and presence (d) of 10 μM calpeptin; (e) shows the average $[\text{Ca}^{2+}]_i$ response from each field of cells.

exposure (≥ 1 h of deregulated calcium for most cells). It was therefore unlikely that NCX3 cleavage could account for DCD in this neuronal population.

Testing the effect of calpeptin on reversible calcium elevations

Cortical neurons were exposed to glutamate (100 μM) plus glycine (10 μM) in the absence of Mg^{2+} for 12 min. This was followed by application of the NMDA and AMPA receptor antagonists MK801 (10 μM) and NBQX (10 μM), respectively, to conclude the glutamate stimulus. Nearly half of neurons maintained calcium homeostasis during and following the 12 min of GluR stimulation, i.e. no large

amplitude increase in Fluo-4FF fluorescence was observed (Fig. 4a). These cells recovered a mitochondrial pattern of TMRM⁺ fluorescence following the addition of GluR antagonists and did not undergo DCD during the subsequent 3 h. A small population of cells exhibited irreversible DCD (Fig. 4b). Numbers of neurons exhibiting each typical behavior are summarized in Fig. 4c.

A substantial fraction of neurons underwent a large DCD-like calcium elevation in response to glutamate that could be reversed following cessation of the stimulation (Fig. 4e–h and Movie S3). These RCE were hallmarked by maintained high $[\text{Ca}^{2+}]_i$ during and often after glutamatergic stimulation followed by recovery of calcium homeostasis at a later time point. Recovery was either sustained (Fig. 4e and f) or followed by DCD (Fig. 4g and h). Some of the cells experienced multiple RCE events prior to DCD (Fig. 4h). TMRM⁺ fluorescence was restored with fast (Fig. 4e) or slow (Fig. 4f) kinetics following the recovery of calcium homeostasis. However, all neurons that failed to recover TMRM⁺ fluorescence following RCE later displayed DCD.

Although cytoplasmic calpain activation became measurable only after a sustained period of DCD, we hypothesized that localized calpain activity below the threshold for detection might be important for converting the DCD-like calcium elevation from a reversible to an irreversible process. Thus, we tested whether addition of calpeptin changed the frequency of RCE following transient GluR stimulation and/or improved recovery from RCE. Calpeptin (10 μM , given together with MK801 and NBQX at the conclusion of GluR stimulation) failed to affect the outcome of the glutamate treatment (Fig. 4c and d).

Evaluation of the chemically distinct calpain inhibitor PD150606

To support the hypothesis that an inhibitory effect of calpeptin on DCD (or RCE) was not masked by non-specific targets, we also tested the chemically unrelated calpain inhibitor PD150606 for protection against DCD. This compound interferes with the calcium binding site rather than the active site of the protease, inhibits purified μ -calpain and m-calpain in the nanomolar range ($K_i = 210$ and 370 nM, respectively), and attenuates α -spectrin breakdown at 1–10 μM in intact cells (Wang *et al.* 1996). As with calpeptin, 10 μM PD150606 did not decrease the incidence of DCD relative to vehicle-treated cultures after 60 min of glutamate treatment although the incidence was slightly reduced at 20 min (only significant for 20% O_2 cultures, Table 1). However, increasing PD150606 to 50 μM , a concentration not specific for calpains (Wang *et al.* 1996; Van den *et al.* 2002), resulted in significant protection of neurons at both 20 and 60 min (Table 1).

To determine whether calpain inhibition was a plausible mechanism for its protective action, we assessed the ability of PD150606 to inhibit α -spectrin breakdown. In contrast to the nearly complete inhibition of α -spectrin cleavage by

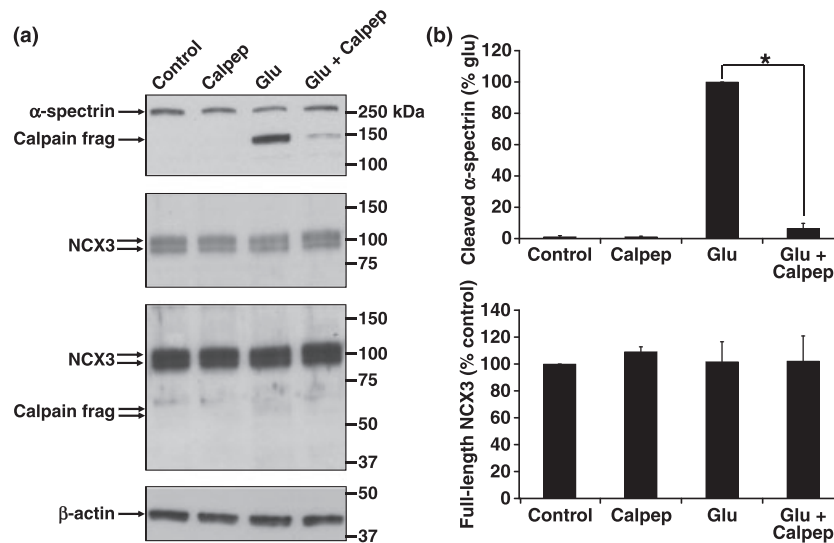


Fig. 3 Calpain-dependent, calpeptin-sensitive processing of α -spectrin but not NCX3. (a) Representative immunoblots depict levels of α -spectrin (first panel) and NCX3 (second and third panels) in whole cell lysates. The third panel is a longer exposure of the second panel. The 150 and 145 kDa calpain cleavage products of α -spectrin are identified while breakdown products of NCX3 relative to full-length NCX3 could

calpeptin, PD150606 even at 50 μ M attenuated α -spectrin breakdown by only $\sim 35\%$ ($n = 3$; Fig. 5). This modest inhibition of calpain activity was unlikely to account for the potent protection of 50 μ M PD150606 against DCD as the $> 90\%$ inhibition of calpain proteolysis by calpeptin was without effect.

The effect of calpeptin on cell death

Although calpain activity was not required for DCD or recovery from RCE in response to 100 μ M glutamate, it remained possible that the late calpain activation occurring ~ 40 min after DCD onset was necessary for the efficient execution of cell death. To address this possibility, we measured the number of healthy, apoptotic, and necrotic neurons at 4, 8, 12, or 20 h after a 30 min excitotoxic glutamate stimulus with or without calpeptin pre-treatment (Fig. 6). PD150606 was not evaluated in this assay because of its limited efficacy as a calpain inhibitor (Fig. 5) and its ability to inhibit multiple calcium-dependent pathways (e.g. Ca^{2+} -calmodulin dependent calcineurin activity; Wang *et al.* 1996). Healthy neurons excluded the apoptosis marker Yo-Pro-1 and the necrosis marker PI from the nucleus and displayed mitochondrial (cytoplasmic) TMRM⁺ fluorescence. Apoptotic neurons were defined as cells with nuclear Yo-Pro-1 fluorescence that excluded PI. Neurons exhibiting nuclear PI fluorescence without cytoplasmic TMRM⁺ fluorescence were considered necrotic.

We observed no significant effect of calpeptin on the number of healthy or necrotic neurons at any of the time

points measured, as assessed by logistic regression analysis (Fig. 6). Apoptotic neurons were not observed at any time point. We also observed no significant effect of calpeptin in parallel assays using cortical neurons cultured at 20% O_2 (data not shown). Thus, cell death in response to 100 μ M glutamate occurred with a normal time-course in the presence of effective calpain inhibition.

Assessing NCX function in acute glutamate excitotoxicity

Finally, although we were unable to detect a significant decrease in full-length NCX3 protein in cortical neurons exposed to glutamate (Fig. 3), it remained possible that a functional loss of NCX activity influenced DCD onset. To assess the workload on the NCX in glutamate-treated cortical neurons, the initial, glutamate-evoked rise of $[\text{Ca}^{2+}]_c$ and $[\text{Na}^+]_c$ and the depolarization of the $\Delta\Psi_P$ were measured using wide-field fluorescence microscopy. To resolve the initial effects and reversibility of the glutamate treatment, a perfusion system was used to deliver glutamate (100 μ M) plus glycine (10 μ M) and to wash out Mg^{2+} .

Figure 7a–c shows the transients of $[\text{Ca}^{2+}]_c$, $[\text{Na}^+]_c$, and $\Delta\Psi_P$ evoked by a 160 s glutamate exposure. Remarkably, the almost instantaneous rise of $[\text{Ca}^{2+}]_c$ (Fig. 7a) and depolarization of the plasma membrane to +10 mV (Fig. 7c) was paralleled by a gradual, high amplitude rise of $[\text{Na}^+]_c$ (Fig. 7b). The large changes in the $[\text{Na}^+]_c$ and $\Delta\Psi_P$ suggested that a forward mode of NCX was not feasible under these circumstances. To quantify the thermodynamic driving force on the NCX, we calculated the ΔG of the forward reaction

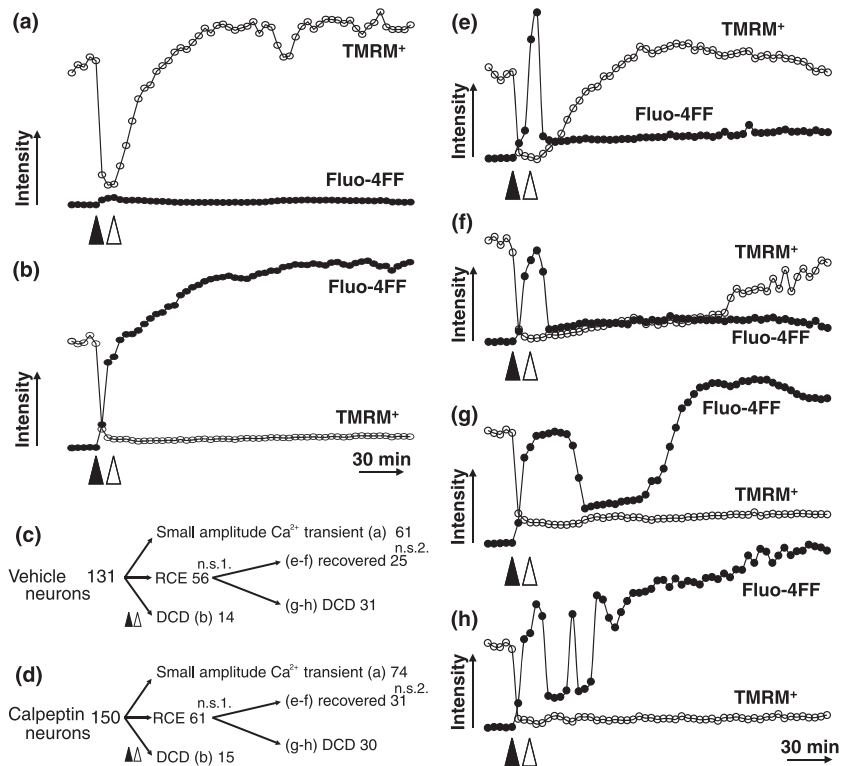


Fig. 4 Reversible calcium elevations (RCE) induced by transient glutamate exposure occurs with variable recovery. TMRM^+ ($-\circ-\circ-$) and Fluo-4FF ($-\bullet-\bullet-$) responses are depicted in representative cells undergoing $[\text{Ca}^{2+}]_c$ changes from four independent experiments. Glutamate ($100 \mu\text{M}$) was added at the solid arrowheads and glutamate receptor activation was terminated by the addition of MK801 ($10 \mu\text{M}$) and NBQX ($10 \mu\text{M}$) after 12 min (open arrowheads). A typical neuron exhibiting a small calcium transient without RCE or DCD is depicted in (a), irreversible DCD is shown in (b), and (e–h) depict cells with RCE.

The cells in (e and f) recover TMRM^+ with fast or slow kinetics, respectively, without subsequent DCD. The cells in (g and h) undergo DCD without TMRM^+ recovery after single (g) or multiple (h) RCE events. The diagrams in (c and d) visualize the total number neurons in each category for vehicle (c) and calpeptin (d; $10 \mu\text{M}$) treated cultures. Data were pooled from four independent experiments; n.s., not significant with Fisher's exact test comparing vehicle and calpeptin treatments and the number of neurons exhibiting RCE (1) or complete recovery (2).

(Ca^{2+} extrusion). The data in Fig. 7d indicate that after addition of glutamate the NCX operated in forward mode for only a very short initial period, during the initial rise of $[\text{Ca}^{2+}]_c$ and before the gross rise of $[\text{Na}^+]_c$. From this time point (< 10 s after glutamate application), the NCX reversed, favoring Ca^{2+} entry, and remained reversed for the entire duration of the experiment ($\Delta G > 0$). While washing out glutamate led to quick re- (and hyper-) polarization of the plasma membrane and close-to-baseline recovery of $[\text{Ca}^{2+}]_c$ (Fig. 7a and c), the elevated $[\text{Na}^+]_c$ (Fig. 7b) supported a maintained reversal of the NCX (Fig. 7d). $[\text{Ca}^{2+}]_c$ did not recover completely to baseline until the end of the experiment likely because of Ca^{2+} influx via the maintained reversal of the NCX (Fig. 7a).

To confirm that the NCX works in reverse during the glutamate-triggered Ca^{2+} plateau, the reverse mode-selective NCX inhibitor KB-R7943 ($10 \mu\text{M}$) was added on top of the glutamate treatment (Fig. 7e). A decrease in $[\text{Ca}^{2+}]_c$ was observed upon addition of KB-R7943. This decrease

suggested that Ca^{2+} entry through reversed NCX contributed to the glutamate-triggered Ca^{2+} plateau. The Ca^{2+} channel blocker nifedipine ($1 \mu\text{M}$) was present in this experiment to exclude the possibility that the effect of KB-R7943 was due to the inhibition of voltage-dependent Ca^{2+} channels (Dietz *et al.* 2007). Remarkably, blocking NCX activity with KB-R7943 decreased the incidence of DCD during a 20 or 60 min glutamate exposure (Table 1). Thus, any inhibition of plasmalemmal NCX function by calpain or other mechanisms would delay rather than promote the induction of DCD in cortical neurons.

Discussion

Calpain proteases play an undisputed but incompletely characterized role in neuronal injury. Calpain inhibitors are protective to varying degrees in animal models of stroke (Bartus *et al.* 1994; Markgraf *et al.* 1998; Tsubokawa *et al.* 2006), traumatic brain injury (Saatman *et al.* 1996; Buki

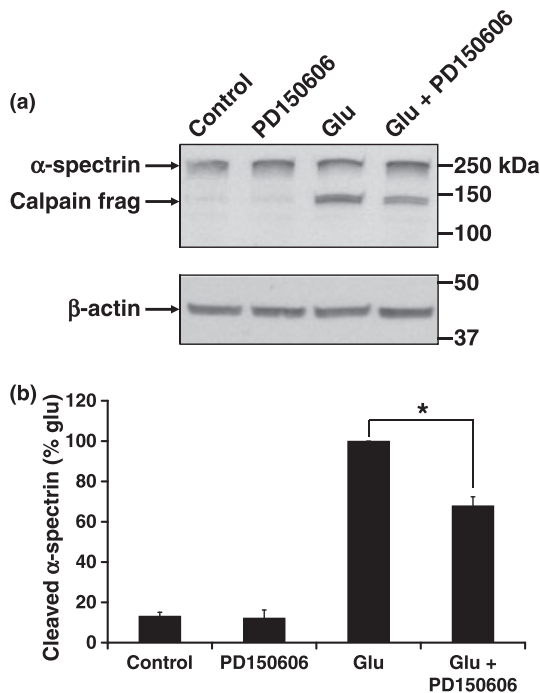


Fig. 5 Inhibition of α -spectrin proteolysis by PD150606. (a) Representative immunoblot depicting full-length and calpain cleaved α -spectrin in whole cell lysate (upper panel), with β -actin as a loading control (lower panel). (b) Densitometric quantification of the results represented in (a) following normalization to β -actin (mean \pm SE, $n = 3$). The asterisk indicates a significant effect of 50 μ M PD150606 + glutamate relative to glutamate alone ($p < 0.05$).

et al. 2003; Ai *et al.* 2007), Alzheimer's disease (Trinchese *et al.* 2008), and Parkinson's disease (Crocker *et al.* 2003). Additionally, calpain-generated α -spectrin breakdown products in CSF are associated with traumatic brain injury severity in humans (Pineda *et al.* 2007). However, despite the early promise of calpain inhibitors, data on long-term outcome in animal studies remain sparse and successful clinical studies in humans have yet to materialize. It is clear that multiple cell death mechanisms contribute to the spatiotemporal profile of neuronal loss *in vivo* and a better understanding of the participation of calpain proteases in the pathogenesis of different injury paradigms is required for the development of targeted treatments. In this study, we set out to (i) identify whether the major activation of calpain proteases in the cytoplasm occurs up or downstream of glutamate-induced intracellular calcium deregulation and (ii) determine whether calpain activity is required for excitotoxic calcium deregulation or cell death in cortical neurons.

Using a genetically encoded calpain sensor, we demonstrated that somal cytoplasmic calpain activity becomes detectable via fluorescent substrate within a very narrowly defined time window at ~ 40 min after the onset of DCD (Fig. 1). Once initiated, cleavage of the FRET sensor

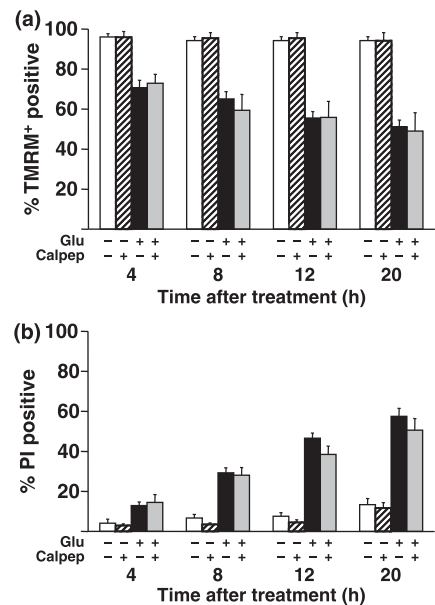
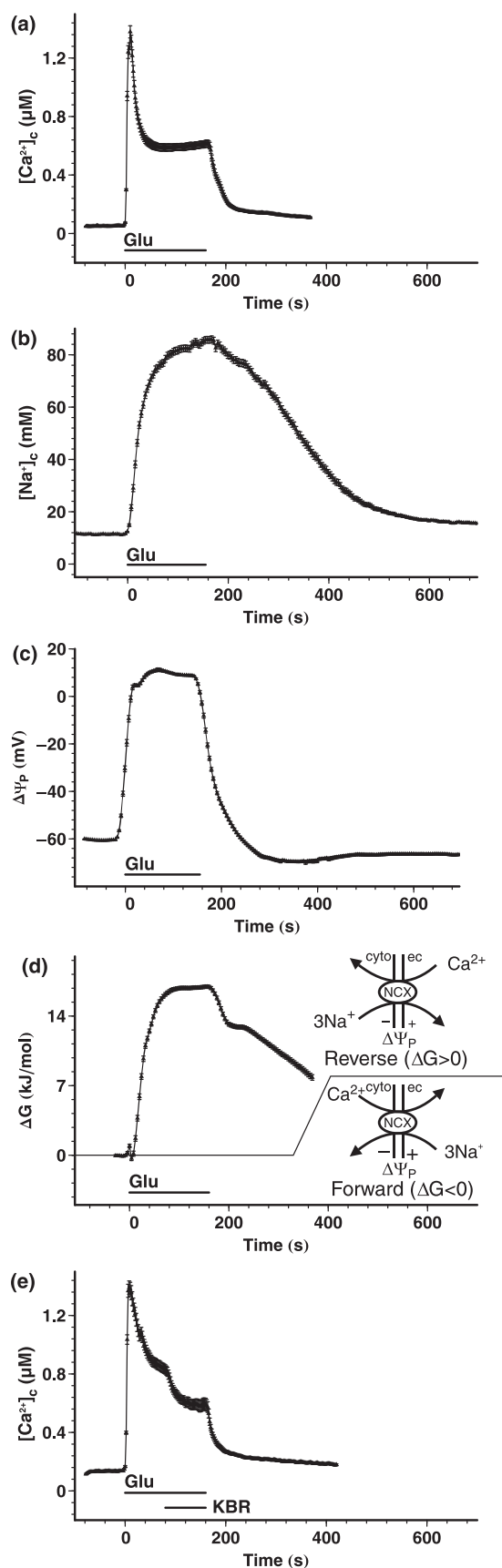


Fig. 6 Effect of calpeptin on cell death following a 30 min glutamate challenge. Cortical neurons received a 30 min 100 μ M glutamate or mock challenge with or without a 30 min calpeptin pre-treatment (white bars, control, hatched bars, calpeptin, black bars, glutamate, gray bars, glutamate + calpeptin). The glutamate challenge was ended by the addition of 10 μ M MK801 + 10 μ M NBQX. Cell viability and death over time were monitored by TMRM⁺ and PI fluorescence, respectively, and quantified at 4, 8, 12, and 20 h after the end of the glutamate challenge. For TMRM⁺ data, mean \pm SE is from $n = 4$ wells for control \pm calpeptin and from $n = 6$ wells for glutamate \pm calpeptin, both from four independent cultures. For PI data, mean \pm SE is from $n = 10$ wells for control \pm calpeptin and from $n = 12$ wells for glutamate \pm calpeptin, both from seven independent cultures. Glutamate and calpeptin were present throughout.

progressed at a constant rate until the loss of FRET was complete (Fig. 1c), suggesting that this event represented 'major' unchecked calpain activation.

The mechanisms of calpain activation in intact neurons are incompletely understood. *In vitro*, both μ -calpain (3–50 μ M) and m-calpain (0.4–0.8 mM) require supra-physiological calcium concentrations for activation (Goll *et al.* 2003). Furthermore, the constitutive expression of an endogenous inhibitor protein, calpastatin, is predicted to limit calpain activity in response to transient pulses of high calcium while ultimately succumbing to proteolysis only if elevated calcium is sustained (Goll *et al.* 2003; Rami 2003). Thus, unchecked calpain activation in neurons is expected only after a period of prolonged calcium deregulation. Our data in Fig. 1 are consistent with a model where the calpastatin-mediated check on calpain activity is relieved following 40 min of sustained DCD, allowing unimpeded calpain proteolysis of cytoplasmic substrates to progress. Because calpain is reportedly sequestered in subcellular membrane fractions including mitochondria (Hewitt *et al.* 1998; Garcia



et al. 2005; Ozaki *et al.* 2007; Kar *et al.* 2008), an alternative possibility is that the delayed but distinct cytoplasmic calpain activation with respect to DCD represents a subcellular translocation event that brings active calpain in contact with the fluorescent sensor.

Spectrin breakdown products and a decrease in FRET were reported in pYSCS-transfected hippocampal neuron dendritic spines within 5 min of glutamate treatment (Vanderklish *et al.* 2000). In our experiments, glutamate treatment of cortical neurons caused an initial calpain-independent, reversible decrease in FRET, suggesting that conformational changes of the probe affect FRET efficiency. While the spectral unmixing and three wavelength FRET calculation avoided errors originating from spectral bleed-through and variations of FRET acceptor fluorescence yield, these calculations also decreased signal-to-noise ratio. Because of the high calpain-insensitive background we cannot confirm or reject the possibility of localized calpain activation (e.g. in subplasma membrane regions) prior to DCD. However, our data do not support a generalized early increase in calpain activity.

The literature on whether calpain activation causatively contributes to GluR-mediated cell death is inconsistent. Early studies found that calpain activity was not required for glutamate excitotoxicity in cerebellar granule (Manev *et al.* 1991) or hippocampal (Adamec *et al.* 1998) neurons, while neuroprotection by calpain inhibitors was reported by others in response to glutamate, kainate, or NMDA (Brorson *et al.* 1995; Rami *et al.* 1997; Lankiewicz *et al.* 2000; Tremblay *et al.* 2000; Araujo *et al.* 2004, 2007; Bano *et al.* 2005; Hou *et al.* 2006; Beart *et al.* 2007; Bevers *et al.* 2009). Although few of these studies addressed the mechanistic involvement of calpains in death, one found that calpain inhibition delayed the late stages of AMPA-induced cortical neuron

Fig. 7 Reversal of the NCX during glutamate treatment of cortical neurons. (a–c) Cortical neurons were wide-field fluorescence imaged to quantify the glutamate-triggered rise of $[Ca^{2+}]_c$ with Fura-4F (a) and in separate experiments the rise of $[Na^+]_c$ (b) and the depolarization of the $\Delta\Psi_p$ (c), using SBFI and PMPI, respectively. Glutamate (100 µM) plus glycine (10 µM) were applied in the absence of Mg^{2+} with a perfusion system (Glu), and then were washed out with Mg^{2+} -containing (1 mM) experimental medium. (d) The thermodynamic driving force of the NCX was calculated from the data shown in (a–c). The $[Ca^{2+}]_e$ and $[Na^+]_e$ were 1.3 mM and 136 mM respectively. A negative ΔG was defined as the forward mode of exchange; i.e. pumping Ca^{2+} out from the cell, while positive ΔG indicates reversal of the NCX. (e) Effect of the reverse-mode NCX inhibitor KB-R7943 (KBR; 10 µM) on the glutamate-triggered $[Ca^{2+}]_c$ plateau. Drug application was performed with a perfusion system with nifedipine (1 µM) continuously present in all perfusion lines. Data are mean \pm SE of neurons pooled from six experiments per condition performed in 3 cell culture preparations ($n = 385, 202, 202,$ and 169 for a, b, c, and d, respectively). The SE in (d) was propagated from (a to c).

death (PI positivity) without preventing early hallmarks of mitochondrial dysfunction (decreased dehydrogenase activity and cytochrome *c* release) (Beart *et al.* 2007). However, another found that over-expression of calpastatin inhibited DCD in cerebellar granule neurons (Bano *et al.* 2005), suggesting an upstream role for calpain involvement in excitotoxic cell death.

Here, we found that calpeptin effectively inhibited calpain-mediated α -spectrin breakdown (Fig. 3) without decreasing the incidence or onset of glutamate-induced DCD (Fig. 2, Table 1). In fact, a small but significant increase in the incidence of DCD was detected when large numbers of neurons were considered, possibly because of inhibition of local calpain processing of NMDA NR2 subunits (Wu *et al.* 2005). Calpeptin was also unable to improve the rate of sustained $[Ca^{2+}]_c$ recovery following glutamate-triggered DCD-like RCE (Fig. 4 and Movie S3), or protect against necrotic cell death (Fig. 6). Apoptotic death was not observed in the present study. Because calpain inhibition protects against neuronal apoptosis (Ray *et al.* 2006; Cao *et al.* 2007), we hypothesize that the percentage of neurons undergoing apoptosis versus necrosis in response to a given excitotoxic challenge ultimately determines the ability of calpain inhibitors to effectively delay GluR-related injury.

Our primary findings contrast with a recent report that over-expression of calpastatin inhibits DCD in cerebellar granule neurons by preventing calpain-mediated NCX3 cleavage (Bano *et al.* 2005). The onset of DCD in cerebellar granule neurons is considerably delayed relative to cortical neurons (e.g. compare Fig. 2 with Bano *et al.* 2005) and it is possible that different mechanisms (apoptotic vs. necrotic) contribute to injury. The expression of NCX3 relative to NCX1 also differs between cortical and cerebellar granule neurons (Kiedrowski *et al.* 2004). We failed to see the appearance of 58–60 kDa NCX3 breakdown products or a degradation of full-length NCX3 in glutamate-treated cortical neurons even after 1.5 h of continuous glutamate treatment (and \sim 1 h after DCD, Fig. 3). The NCX antagonist KB-R7943 delayed rather than shortened the time to DCD (Table 1), suggesting that in our model NCX activity following glutamate exposure was deleterious rather than protective. Calculation of the ΔG for NCX (Fig. 7) revealed that NCX operates in reverse mode favoring Ca^{2+} entry during glutamate exposure, in agreement with previous reports (Kiedrowski *et al.* 1994, 2004; Hoyt *et al.* 1998; Czyz and Kiedrowski 2002; Araujo *et al.* 2007; Storozhevych *et al.* 2007). Consistent with reverse mode NCX operation, KB-R7943 acutely decreased intracellular Ca^{2+} when administered after glutamate addition (Fig. 7e). Thus, NCX failure cannot explain the sudden loss of calcium homeostasis in glutamate-exposed cortical neurons although failure of other calcium extrusion pathways (e.g. the plasma membrane calcium ATPase; Pottorf *et al.* 2006) may contribute.

In summary, our studies for the first time imaged somal calpain activation relative to intracellular calcium changes in live glutamate-treated neurons, revealing the onset of major activity following \sim 40 min of sustained DCD. Modifications of this technique, particularly ones that reduce pH-sensitive and calpeptin-insensitive changes in fluorescence, should be useful for characterizing calpain activation in less acute models of neuronal injury where calpain inhibitors are protective.

Acknowledgements

We thank Richard Oh for the preparation of primary cortical neurons, Dr Ken Philipson for generously providing NCX3 antibody, and Dr Peter Vanderklish for kindly providing the pYSCS plasmid. This study was supported by NIH Grants PL1 AG032118 and P30 AG025708 at the Buck Institute and by NIH Grant NS054764 to BMP.

Supporting information

Additional Supporting information may be found in the online version of this article:

Appendix S1. Materials and methods

Movie S1. Delayed calcium deregulation. “Fura6F.avi” depicts the Fura-6F ratio image series in Fig. 1a. Warmer colors represent higher $[Ca^{2+}]_c$. Red indicates DCD. The original frame interval was 2 min. Glutamate was added after frame number 10.

Movie S2. Calpain activation. “pYSCS.avi” depicts the calpain sensor FRET image series in Fig. 1b. Warmer colors represent higher FRET. Blue pseudocolor indicates loss of FRET and calpain activation. The original frame interval was 2 min. Glutamate was added after frame number 10.

Movie S3 Reversible calcium elevations. “RCE.avi” shows a field of 8 neurons loaded with TMRM⁺ (red) and Fluo-4FF (green), depicting Fig. 4. Four of eight neurons displayed RCE in response to transient glutamate receptor stimulation. An arrowhead denotes one of these cells that underwent subsequent DCD, while a recovering cell is indicated by an arrow. “Glu” denotes frames when glutamate receptors were stimulated. The original frame interval was 4 min.

Please note: Wiley-Blackwell are not responsible for the content or functionality of any supporting materials supplied by the authors. Any queries (other than missing material) should be directed to the corresponding author for the article.

References

- Adamec E., Beermann M. L. and Nixon R. A. (1998) Calpain I activation in rat hippocampal neurons in culture is NMDA receptor selective and not essential for excitotoxic cell death. *Brain Res. Mol. Brain Res.* **54**, 35–48.
- Ai J., Liu E., Wang J., Chen Y., Yu J. and Baker A. J. (2007) Calpain inhibitor MDL-28170 reduces the functional and structural deterioration of corpus callosum following fluid percussion injury. *J. Neurotrauma* **24**, 960–978.
- Araujo I. M., Verdasca M. J., Leal E. C., Bahr B. A., Ambrosio A. F., Carvalho A. P. and Carvalho C. M. (2004) Early calpain-mediated

- proteolysis following AMPA receptor activation compromises neuronal survival in cultured hippocampal neurons. *J. Neurochem.* **91**, 1322–1331.
- Araujo I. M., Carreira B. P., Pereira T., Santos P. F., Soulet D., Inacio A., Bahr B. A., Carvalho A. P., Ambrosio A. F. and Carvalho C. M. (2007) Changes in calcium dynamics following the reversal of the sodium-calcium exchanger have a key role in AMPA receptor-mediated neurodegeneration via calpain activation in hippocampal neurons. *Cell Death Differ.* **14**, 1635–1646.
- Bano D., Young K. W., Guerin C. J., Lefevre R., Rothwell N. J., Naldini L., Rizzuto R., Carafoli E. and Nicotera P. (2005) Cleavage of the plasma membrane Na⁺/Ca²⁺ exchanger in excitotoxicity. *Cell* **120**, 275–285.
- Bartus R. T., Hayward N. J., Elliott P. J., Sawyer S. D., Baker K. L., Dean R. L., Akiyama A., Straub J. A., Harbeson S. L. and Li Z. (1994) Calpain inhibitor AK295 protects neurons from focal brain ischemia. Effects of postocclusion intra-arterial administration. *Stroke* **25**, 2265–2270.
- Beart P. M., Lim M. L., Chen B., Diwakarla S., Mercer L. D., Cheung N. S. and Nagley P. (2007) Hierarchical recruitment by AMPA but not staurosporine of pro-apoptotic mitochondrial signaling in cultured cortical neurons: evidence for caspase-dependent/independent cross-talk. *J. Neurochem.* **103**, 2408–2427.
- Bers D. M. and Ginsburg K. S. (2007) Na:Ca stoichiometry and cytosolic Ca-dependent activation of NCX in intact cardiomyocytes. *Ann. NY Acad. Sci.* **1099**, 326–338.
- Beyers M. B. and Neumar R. W. (2008) Mechanistic role of calpains in postischemic neurodegeneration. *J. Cereb. Blood Flow Metab.* **28**, 655–673.
- Beyers M. B., Lawrence E., Maronski M., Starr N., Amesquita M. and Neumar R. W. (2009) Knockdown of m-calpain increases survival of primary hippocampal neurons following NMDA excitotoxicity. *J. Neurochem.* **108**, 1237–1250.
- Blaustein M. P. and Lederer W. J. (1999) Sodium/calcium exchange: its physiological implications. *Physiol. Rev.* **79**, 763–854.
- Bolshakov A. P., Mikhailova M. M., Szabadkai G., Pinelis V. G., Brustovetsky N., Rizzuto R. and Khodorov B. I. (2008) Measurements of mitochondrial pH in cultured cortical neurons clarify contribution of mitochondrial pore to the mechanism of glutamate-induced delayed Ca²⁺ deregulation. *Cell Calcium* **43**, 602–614.
- Bredesen D. E., Rao R. V. and Mehlen P. (2006) Cell death in the nervous system. *Nature* **443**, 796–802.
- Brorson J. R., Marcuccilli C. J. and Miller R. J. (1995) Delayed antagonism of calpain reduces excitotoxicity in cultured neurons. *Stroke* **26**, 1259–1266.
- Buki A., Farkas O., Doczi T. and Povlishock J. T. (2003) Preinjury administration of the calpain inhibitor MDL-28170 attenuates traumatically induced axonal injury. *J. Neurotrauma* **20**, 261–268.
- Cao G., Xing J., Xiao X., Liou A. K., Gao Y., Yin X. M., Clark R. S., Graham S. H. and Chen J. (2007) Critical role of calpain I in mitochondrial release of apoptosis-inducing factor in ischemic neuronal injury. *J. Neurosci.* **27**, 9278–9293.
- Castilho R. F., Hansson O., Ward M. W., Budd S. L. and Nicholls D. G. (1998) Mitochondrial control of acute glutamate excitotoxicity in cultured cerebellar granule cells. *J. Neurosci.* **18**, 10277–10286.
- Crocker S. J., Smith P. D., Jackson-Lewis V. et al. (2003) Inhibition of calpains prevents neuronal and behavioral deficits in an MPTP mouse model of Parkinson's disease. *J. Neurosci.* **23**, 4081–4091.
- Czyz A. and Kiedrowski L. (2002) In depolarized and glucose-deprived neurons, Na⁺ influx reverses plasmalemmal K⁺-dependent and K⁺-independent Na⁺/Ca²⁺ exchangers and contributes to NMDA excitotoxicity. *J. Neurochem.* **83**, 1321–1328.
- Dietz R. M., Kiedrowski L. and Shuttleworth C. W. (2007) Contribution of Na⁺/Ca²⁺ exchange to excessive Ca²⁺ loading in dendrites and somata of CA1 neurons in acute slice. *Hippocampus* **17**, 1049–1059.
- Friedrich P. (2004) The intriguing Ca²⁺ requirement of calpain activation. *Biochem. Biophys. Res. Commun.* **323**, 1131–1133.
- Garcia M., Bondada V. and Geddes J. W. (2005) Mitochondrial localization of mu-calpain. *Biochem. Biophys. Res. Commun.* **338**, 1241–1247.
- Gerencser A. A. and Adam-Vizi V. (2005) Mitochondrial Ca²⁺ dynamics reveals limited intramitochondrial Ca²⁺ diffusion. *Biophys. J.* **88**, 698–714.
- Gerencser A. A. and Nicholls D. G. (2008) Measurement of instantaneous velocity vectors of organelle transport: mitochondrial transport and bioenergetics in hippocampal neurons. *Biophys. J.* **95**, 3079–3099.
- Gerencser A. A., Doczi J., Torocsik B., Bossy-Wetzel E. and Adam-Vizi V. (2008) Mitochondrial swelling measurement in situ by optimized spatial filtering: astrocyte–neuron differences. *Biophys. J.* **95**, 2583–2598.
- Goll D. E., Thompson V. F., Li H., Wei W. and Cong J. (2003) The calpain system. *Physiol. Rev.* **83**, 731–801.
- Grote J., Laue O., Eiring P. and Wehler M. (1996) Evaluation of brain tissue O₂ supply based on results of PO₂ measurements with needle and surface microelectrodes. *J. Auton. Nerv. Syst.* **57**, 168–172.
- Grynkiwicz G., Poenie M. and Tsien R. Y. (1985) A new generation of Ca²⁺ indicators with greatly improved fluorescence properties. *J. Biol. Chem.* **260**, 3440–3450.
- Guttmann R. P., Sokol S., Baker D. L., Simpkins K. L., Dong Y. and Lynch D. R. (2002) Proteolysis of the N-methyl-D-aspartate receptor by calpain in situ. *J. Pharmacol. Exp. Ther.* **302**, 1023–1030.
- Hewitt K. E., Lesiuk H. J., Tauskela J. S., Morley P. and Durkin J. P. (1998) Selective coupling of mu-calpain activation with the NMDA receptor is independent of translocation and autolysis in primary cortical neurons. *J. Neurosci. Res.* **54**, 223–232.
- Hou S. T., Jiang S. X., Desbois A., Huang D., Kelly J., Tessier L., Karchewski L. and Kappler J. (2006) Calpain-cleaved collapsin response mediator protein-3 induces neuronal death after glutamate toxicity and cerebral ischemia. *J. Neurosci.* **26**, 2241–2249.
- Hoyt K. R., Arden S. R., Aizenman E. and Reynolds I. J. (1998) Reverse Na⁺/Ca²⁺ exchange contributes to glutamate-induced intracellular Ca²⁺ concentration increases in cultured rat forebrain neurons. *Mol. Pharmacol.* **53**, 742–749.
- Kar P., Chakraborti T., Samanta K. and Chakraborti S. (2008) Submitochondrial localization of associated mu-calpain and calpastatin. *Arch. Biochem. Biophys.* **470**, 176–186.
- Kiedrowski L., Brooker G., Costa E. and Wroblewski J. T. (1994) Glutamate impairs neuronal calcium extrusion while reducing sodium gradient. *Neuron* **12**, 295–300.
- Kiedrowski L., Czyz A., Baranauskas G., Li X. F. and Lytton J. (2004) Differential contribution of plasmalemmal Na/Ca exchange isoforms to sodium-dependent calcium influx and NMDA excitotoxicity in depolarized neurons. *J. Neurochem.* **90**, 117–128.
- Lankiewicz S., Marc L. C., Truc B. N., Krohn A. J., Poppe M., Cole G. M., Saido T. C. and Prehn J. H. (2000) Activation of calpain I converts excitotoxic neuron death into a caspase-independent cell death. *J. Biol. Chem.* **275**, 17064–17071.
- Lee M. S., Kwon Y. T., Li M., Peng J., Friedlander R. M. and Tsai L. H. (2000) Neurotoxicity induces cleavage of p35 to p25 by calpain. *Nature* **405**, 360–364.
- Lin M. T. and Beal M. F. (2006) Mitochondrial dysfunction and oxidative stress in neurodegenerative diseases. *Nature* **443**, 787–795.
- Manev H., Favaron M., Siman R., Guidotti A. and Costa E. (1991) Glutamate neurotoxicity is independent of calpain I inhibition in

- primary cultures of cerebellar granule cells. *J. Neurochem.* **57**, 1288–1295.
- Markgraf C. G., Velayo N. L., Johnson M. P., McCarty D. R., Medhi S., Koehl J. R., Chmielewski P. A. and Linnik M. D. (1998) Six-hour window of opportunity for calpain inhibition in focal cerebral ischemia in rats. *Stroke* **29**, 152–158.
- Nicholls D. G. (2004) Mitochondrial dysfunction and glutamate excitotoxicity studied in primary neuronal cultures. *Curr. Mol. Med.* **4**, 149–177.
- Nicholls D. G. (2006) Simultaneous monitoring of ionophore- and inhibitor-mediated plasma and mitochondrial membrane potential changes in cultured neurons. *J. Biol. Chem.* **281**, 14864–14874.
- Ozaki T., Tomita H., Tamai M. and Ishiguro S. (2007) Characteristics of mitochondrial calpains. *J. Biochem.* **142**, 365–376.
- Pineda J. A., Lewis S. B., Valadka A. B. *et al.* (2007) Clinical significance of alphaII-spectrin breakdown products in cerebrospinal fluid after severe traumatic brain injury. *J. Neurotrauma* **24**, 354–366.
- Polster B. M., Basanez G., Etzebarria A., Hardwick J. M. and Nicholls D. G. (2005) Calpain I induces cleavage and release of apoptosis-inducing factor from isolated mitochondria. *J. Biol. Chem.* **280**, 6447–6454.
- Pottorf W. J., Johanns T. M., Derrington S. M., Strehler E. E., Enyedi A. and Thayer S. A. (2006) Glutamate-induced protease-mediated loss of plasma membrane Ca pump activity in rat hippocampal neurons. *J. Neurochem.* **98**, 1646–1656.
- Rami A. (2003) Ischemic neuronal death in the rat hippocampus: the calpain-calpastatin-caspase hypothesis. *Neurobiol. Dis.* **13**, 75–88.
- Rami A., Ferger D. and Kriegstein J. (1997) Blockade of calpain proteolytic activity rescues neurons from glutamate excitotoxicity. *Neurosci. Res.* **27**, 93–97.
- Randall R. D. and Thayer S. A. (1992) Glutamate-induced calcium transient triggers delayed calcium overload and neurotoxicity in rat hippocampal neurons. *J. Neurosci.* **12**, 1882–1895.
- Ray S. K., Karmakar S., Nowak M. W. and Banik N. L. (2006) Inhibition of calpain and caspase-3 prevented apoptosis and preserved electrophysiological properties of voltage-gated and ligand-gated ion channels in rat primary cortical neurons exposed to glutamate. *Neurosci* **139**, 577–595.
- Saatman K. E., Murai H., Bartus R. T., Smith D. H., Hayward N. J., Perri B. R. and McIntosh T. K. (1996) Calpain inhibitor AK295 attenuates motor and cognitive deficits following experimental brain injury in the rat. *Proc. Natl Acad. Sci. USA* **93**, 3428–3433.
- Siman R. and Noszek J. C. (1988) Excitatory amino acids activate calpain I and induce structural protein breakdown in vivo. *Neuron* **1**, 279–287.
- Simpkins K. L., Guttman R. P., Dong Y., Chen Z., Sokol S., Neumar R. W. and Lynch D. R. (2003) Selective activation induced cleavage of the NR2B subunit by calpain. *J. Neurosci.* **23**, 11322–11331.
- Slemmer J. E., Matsushita S., De Zeeuw C. I., Weber J. T. and Knopfel T. (2004) Glutamate-induced elevations in intracellular chloride concentration in hippocampal cell cultures derived from EYFP-expressing mice. *Eur. J. Neurosci.* **19**, 2915–2922.
- Springer J. E., Azbill R. D., Kennedy S. E., George J. and Geddes J. W. (1997) Rapid calpain I activation and cytoskeletal protein degradation following traumatic spinal cord injury: attenuation with riluzole pretreatment. *J. Neurochem.* **69**, 1592–1600.
- Storozhevych T. P., Sorokina E. G., Vabnitz A. V., Senilova Y. E., Tukhbatova G. R. and Pinelis V. G. (2007) Na⁺/Ca²⁺ exchange and regulation of cytoplasmic concentration of calcium in rat cerebellar neurons treated with glutamate. *Biochemistry (Mosc)* **72**, 750–759.
- Stout A. K., Raphael H. M., Kanterewicz B. I., Klann E. and Reynolds I. J. (1998) Glutamate-induced neuron death requires mitochondrial calcium uptake. *Nat. Neurosci.* **1**, 366–373.
- Tremblay R., Chakravarthy B., Hewitt K., Tauskela J., Morley P., Atkinson T. and Durkin J. P. (2000) Transient NMDA receptor inactivation provides long-term protection to cultured cortical neurons from a variety of death signals. *J. Neurosci.* **20**, 7183–7192.
- Trinchese F., Fa⁺ M., Liu S. *et al.* (2008) Inhibition of calpains improves memory and synaptic transmission in a mouse model of Alzheimer disease. *J. Clin. Invest.* **118**, 2796–2807.
- Tsubokawa T., Yamaguchi-Okada M., Calvert J. W., Solaroglu I., Shimamura N., Yata K. and Zhang J. H. (2006) Neurovascular and neuronal protection by E64d after focal cerebral ischemia in rats. *J. Neurosci. Res.* **84**, 832–840.
- Van den B. L., Van D. P., Vleminckx V., Van H. E., Lemmens G., Missiaen L., Callewaert G. and Robberecht W. (2002) An alpha-mercaptoacrylic acid derivative (PD150606) inhibits selective motor neuron death via inhibition of kainate-induced Ca²⁺ influx and not via calpain inhibition. *Neuropharmacology* **42**, 706–713.
- Vanderklish P. W., Krushel L. A., Holst B. H., Gally J. A., Crossin K. L. and Edelman G. M. (2000) Marking synaptic activity in dendritic spines with a calpain substrate exhibiting fluorescence resonance energy transfer. *Proc. Natl Acad. Sci. USA* **97**, 2253–2258.
- Vergun O., Keelan J., Khodorov B. I. and Duchon M. R. (1999) Glutamate-induced mitochondrial depolarisation and perturbation of calcium homeostasis in cultured rat hippocampal neurones. *J. Physiol.* **519** Pt 2, 451–466.
- Vesce S., Kirk L. and Nicholls D. G. (2004) Relationships between superoxide levels and delayed calcium deregulation in cultured cerebellar granule cells exposed continuously to glutamate. *J. Neurochem.* **90**, 683–693.
- Wang K. K., Nath R., Posner A. *et al.* (1996) An alpha-mercaptoacrylic acid derivative is a selective nonpeptide cell-permeable calpain inhibitor and is neuroprotective. *Proc. Natl Acad. Sci. USA* **93**, 6687–6692.
- Wu M. L., Chen J. H., Chen W. H., Chen Y. J. and Chu K. C. (1999) Novel role of the Ca(2+)-ATPase in NMDA-induced intracellular acidification. *Am. J. Physiol.* **277**, C717–C727.
- Wu H. Y., Tomizawa K., Oda Y., Wei F. Y., Lu Y. F., Matsushita M., Li S. T., Moriwaki A. and Matsui H. (2004) Critical role of calpain-mediated cleavage of calcineurin in excitotoxic neurodegeneration. *J. Biol. Chem.* **279**, 4929–4940.
- Wu H. Y., Yuen E. Y., Lu Y. F., Matsushita M., Matsui H., Yan Z. and Tomizawa K. (2005) Regulation of NMDA receptors by calpain in cortical neurons. *J. Biol. Chem.* **280**, 21588–21593.
- Xu W., Wong T. P., Chery N., Gaertner T., Wang Y. T. and Baudry M. (2007) Calpain-mediated mGluR1alpha truncation: a key step in excitotoxicity. *Neuron* **53**, 399–412.
- Yuen E. Y., Gu Z. and Yan Z. (2007a) Calpain regulation of AMPA receptor channels in cortical pyramidal neurons. *J. Physiol.* **580**, 241–254.
- Yuen E. Y., Liu W. and Yan Z. (2007b) The phosphorylation state of GluR1 subunits determines the susceptibility of AMPA receptors to calpain cleavage. *J. Biol. Chem.* **282**, 16434–16440.
- Zhang J., Campbell R. E., Ting A. Y. and Tsien R. Y. (2002) Creating new fluorescent probes for cell biology. *Nat. Rev. Mol. Cell Biol.* **3**, 906–918.